

Cost Effective Computationally Intelligent Control – An Augmented Switching Manifold Approach

Mehmet Önder Efe
Carnegie Mellon University
Electrical and Computer Engineering Department
Pittsburgh, PA 15213-3890
U.S.A.
efemond@andrew.cmu.edu

Xinghuo Yu
Central Queensland University
Faculty of Informatics and Communication
Rockhampton, QLD 4702
AUSTRALIA
X.Yu@cqu.edu.au

Okyay Kaynak
Bogazici University
Electrical and Electronic Engineering Department
Bebek, 80815, Istanbul
TURKEY
kaynak@boun.edu.tr

Serdar Iplikçi
Bogazici University
Electrical and Electronic Engineering Department
Bebek, 80815, Istanbul
TURKEY
iplikcis@boun.edu.tr

Abstract - In this paper, a novel method for tuning the parameters of a class of intelligent PD controllers is discussed. The aim of the design is to extract a tuning law such that the specifications of the control problem are met and the adjustable parameters evolve bounded. The achievement of these specifications is a challenge in the presence of strong external disturbances, ambiguities in the plant model and nonlinearities, which absolutely require robustness for performance and stability for safety and applicability. The approach introduced in this paper achieves these targets by utilizing the sliding mode control technique based on an augmented switching manifold. The proposed law is applicable to the class of controllers, the output of each member of which is linear in the adjustable parameter set. This stipulates that the application spectrum of the algorithm extends from PID controller to fuzzy controllers and some structures of neural controllers. In the application example, control of a coupled double pendulum system is considered. The dynamic model of the plant is assumed to be unknown and the difficulties introduced by observation noise are studied.

I. INTRODUCTION

The problem of tuning the parameters of a controller for meeting a set of predefined performance specifications is a challenge because of the nonlinearities existing in the plant model, disturbances and time varying nature of the processes. Especially if the accuracy in the response is sought, the controller must have a degree of robustified intelligence so that the nonlinear behavior is handled together with disturbance rejection ability. One must now question how the designer can define robustified intelligence and achieve it with the known design tools. The concept of intelligence in this context should refer to the acquisition of the current state of the system under investigation and generating an appropriate decision with an increased autonomy. In this respect, the design of a training strategy necessitates the separation of useful knowledge and disturbance related components contained in the training signals, which directly influence the evolution of the parameters and consequently the output of the intelligent system. Robustified intelligence accounts for the behavior in the parameter space, the motions

in which are characterized by the adopted training strategy; and the robustness in this space can be defined as the occurrence of a parametric evolution in finite volume.

The studies reporting the use of Sliding Mode Control (SMC) for parameter tuning in Computational Intelligence (CI) by Sanner and Slotine [1], and Sira-Ramirez and Colina-Morles [2] have been the stimulants, which proved that the robustness feature of SMC could be exploited in the training of the architectures of CI. These studies pioneered a vast majority of researchers working on SMC and CI. Sanner and Slotine considered the training of GRBFNN which has certain degrees of analytical tractability in explaining the stability issues, and Sira-Ramirez et al have shown the use of ADALINEs with a SMC based learning strategy. As an illustrative example, the inverse dynamics identification of a Kapitsa pendulum has been demonstrated together with a thorough analysis towards the handling of disturbances. Hsu and Real [3-4] demonstrate the use of SMC with Gaussian NNs, Yu et al [5] introduces the dynamic uncertainty adaptation of what is proposed in [2], and demonstrate the performance of the scheme on the Kapitsa pendulum. Parma et al [6] use the SMC technique in parameter tuning process of multilayer perceptron. Latest studies towards the integration of SMC and CI have shown that the tuning can be implemented in dynamic weight filter neurons [7] and in parameters of a controller [8]. A different viewpoint towards this integration is due to Efe et al [9-10], which has the goal of reducing the adverse effects of noise driven parameter tuning activity in gradient techniques. The key idea in these works is the mix two training signals in a weighted average sense. A good deal of review is provided in the recent survey of Kaynak et al [11]. The survey illustrates how SMC can be used for training in CI as well as how CI can be utilized for the tuning of parameters in conventional SMC.

In [8,12], it is presented that the original form of the method discussed by Ramirez et al [2] can be used for control applications, in which the target output of the intelligent system, i.e. the controller, is unknown. The major difference of what is presented in this paper from what has been discussed in the literature is the construction of a

dynamic adaptation law based on a switching manifold, which is augmented with the sensitivity derivatives of an appropriately defined cost function. The paper analyzes the relation between the sliding surface for the plant to be controlled and the zero learning error level for the output of a flexible controller.

The organization of the paper is as follows: The second section gives the definitions and the formulation of the problem and derives the first critical value of the uncertainty bound parameter denoted by K . The following section introduces the equivalence constraints on the sliding control performance for the plant and sliding mode learning performance for the controller. The section gives the second critical value of K and combines the two constraints. The fourth section describes the dynamic model of the plant used in the simulations and presents the simulation studies. Conclusions constitute the last part of the paper.

II. PARAMETER TUNING BASED ON A TWO-TERM LYAPUNOV FUNCTION

In this section, an analysis of the sliding mode creation problem, which is based on a two-term Lyapunov function, is given. The proposed form of the update dynamics constructs the time derivative of the parameter vector, the use of which results in the observation of a sliding mode taking place after a reaching mode on the phase plane.

Consider the 3-input single output controller structure described as

$$\tau = \underline{\phi}^T \underline{u}_A \quad (1)$$

where,

$$\underline{\phi} = [\phi_1 \quad \phi_2 \quad \phi_3]^T \quad (2)$$

$$\underline{u}_A = [u_1 \quad u_2 \quad 1]^T = [e \quad \dot{e} \quad 1]^T \quad (3)$$

In above, the symbol e denotes the tracking error, which is the discrepancy between the response of the system under control (x) and the reference signal (x_d), i.e. $e = x - x_d$. The structure of the control system is an ordinary feedback loop as illustrated in Fig. 1. The definitions of the sliding line s_p and that of zero learning-error level s_c , which are seen in this figure, are described as

$$s_p(e, \dot{e}) = \dot{e} + \lambda e \quad (4)$$

where, λ is the slope of the sliding surface and

$$s_c(\tau, \tau_d) = \tau - \tau_d \quad (5)$$

where, τ_d is the desired output of the controller and is unknown. Based on these definitions, one can define the following quantity as the cost measure,

$$J = \frac{1}{2} s_c^2 \quad (6)$$

which instantly qualifies the similarity between the produced control signal and its desired value. Using this measure, an augmented switching manifold can be designed as in (7), and a Lyapunov function can be constructed as in (8).

$$\underline{s}_A = \begin{bmatrix} s_c \\ \frac{\partial J}{\partial \underline{\phi}} \end{bmatrix} \quad (7)$$

$$V_c = \frac{1}{2} \underline{s}_A^T P \underline{s}_A \quad (8)$$

where, P is defined as follows.

$$P = \begin{bmatrix} \mu & \underline{0}_{1 \times (m+1)} \\ \underline{0}_{(m+1) \times 1} & \rho I_{(m+1) \times (m+1)} \end{bmatrix} \quad (9)$$

where, μ and ρ are positive constants. Based on the selection in (9), the open form of the Lyapunov function in (10) can be written as follows.

$$V_c = \mu J + \rho \frac{1}{2} \left\| \frac{\partial J}{\partial \underline{\phi}} \right\|^2 \quad (10)$$

in which, the selection of the weight parameters μ and ρ must be done by comparing the magnitudes of the time-varying two terms of (10). For a vector denoted by \underline{v} , the definition of the norm used in (10) can be given as $\|\underline{v}\| = (\underline{v}^T \underline{v})^{1/2}$.

In order not to violate the constraints of the physical reality, the following bound conditions are imposed.

$$\|\underline{\phi}\| \leq B_\phi \quad (11)$$

$$\|\underline{u}_A\| \leq B_{u_A} \quad (12)$$

$$\|\dot{\underline{u}}_A\| \leq B_{\dot{u}_A} \quad (13)$$

$$\|\tau\| \leq B_\tau \quad (14)$$

$$\|\tau_d\| \leq B_{\tau_d} \quad (15)$$

$$\|\dot{\tau}_d\| \leq B_{\dot{\tau}_d} \quad (16)$$

The numerical values of these bounds are not certain in most of the applications but the realistic design approaches must take them into consideration as they determine the domain of applicability of a strategy.

Theorem 1. For a controller structure, in which the output is a linear function of the adjustable parameters, the adaptation of the controller parameters as described in (17) ensures the negative definiteness of the time derivative of the Lyapunov function candidate in (10).

$$\dot{\underline{\phi}} = -K \left(\mu I + \rho \frac{\partial^2 J}{\partial \underline{\phi} \partial \underline{\phi}^T} \right)^{-1} \text{sgn} \left(\frac{\partial J}{\partial \underline{\phi}} \right) \quad (17)$$

where, K is a sufficiently large constant satisfying (18).

$$K > K_{cr1} = (\mu B_{\phi} + \rho B_{u_A}) B_{\dot{u}_A} \quad (18)$$

where, K_{cr1} is the first critical lower bound of the uncertainty bound parameter K . (Proof of the theorem is omitted due to the space limit, the details can be found in [12].)

III. ANALYSIS OF THE EQUIVALENCE BETWEEN SLIDING MODE CONTROL AND SLIDING MODE LEARNING

Consider the sliding line s_p and the zero-learning-error level s_c described by (4) and (5) respectively. The relation between these two quantities is assumed as in (19).

$$s_c = \Psi(s_p) \quad (19)$$

Qualitatively, if the value of s_p tends to zero, this means that s_c goes to zero. Theoretically, the system achieves perfect tracking because the controller produces the desired control inputs or vice versa. Conversely, as the value of s_p increases in magnitude, indicating that the error vector is getting away from the origin, the same sort of a divergent behavior in s_c is observed or vice versa. The details in postulating the form of the relation Ψ are presented in [8].

Theorem 2. All monotonically increasing continuous functions passing through the origin can serve as the Ψ relation for the establishment of an equivalence between the sliding mode control of the plant and the sliding mode learning inside the controller.

$$\begin{aligned} \dot{V}_p &= \dot{s}_p s_p \\ &= (\Psi^{-1}(s_c)) \dot{\Psi}^{-1}(s_c) \\ &= \frac{\partial \Psi^{-1}(s_c)}{\partial s_c} \dot{s}_c \Psi^{-1}(s_c) \\ &= \frac{\partial \Psi^{-1}(s_c)}{\partial s_c} \left(\dot{\phi}^T \underline{u}_A + \dot{\phi}^T \underline{\dot{u}}_A - \dot{\tau}_d \right) \Psi^{-1}(s_c) \\ &\leq \frac{\partial \Psi^{-1}(s_c)}{\partial s_c} \left| \Psi^{-1}(s_c) \right|^* \\ &\quad \left((B_{\phi} B_{\dot{u}_A} + B_{\tau_d}) - \frac{K}{\mu + \rho B_{u_A}^2} \right) \\ &< 0 \Leftrightarrow K > K_{cr2} = (B_{\phi} B_{\dot{u}_A} + B_{\tau_d}) (\mu + \rho B_{u_A}^2) \end{aligned} \quad (20)$$

It is now clear that there are two critical lower bound values for the uncertainty bound parameter K , and the formulation of these values are seen in (18) for K_{cr1} , and in the last line of (20) for K_{cr2} . In (21), the two constraints on the design parameter K are combined.

$$K > \max(K_{cr1}, K_{cr2}) \quad (21)$$

Apparently the selection of the bound parameter as given in (21) enforces the value of s_c to zero level, or equivalently, s_p to zero.

IV. SIMULATION STUDIES

In this study, a coupled double pendulum system is used to elaborate the performance of the method discussed. The physical structure of the plant is illustrated in Fig. 2. Since the dynamics of such a mechatronic system is modeled by nonlinear and coupled differential equations, precise tracking becomes a difficult objective due to the strong interdependency between the variables involved. Furthermore, the ambiguities introduced by the noise on the measured quantities make the design of a robust controller so complicated that the achievement of which is a challenge in conventional design framework. Therefore, for such a system, the control methodology adopted must be capable of handling the difficulties stated.

The differential equations characterizing the behavior of the system are given in (22)-(25), in which the angular positions and the angular velocities define the state vector. The control inputs, which are denoted by τ_1 and τ_2 , are provided to the relevant pendulum by the base servomotors. The parameters of the plant are given in Table 1.

$$\dot{x}_1 = x_3 \quad (22)$$

$$\dot{x}_2 = x_4 \quad (23)$$

$$\dot{x}_3 = \left(\frac{M_1 g r}{J_1} - \frac{k_s r^2}{4J_1} \right) \sin(x_1) + \quad (24)$$

$$\frac{k_s r}{2J_1} (l-b) + \frac{\tau_1}{J_1} + \frac{k_s r^2}{4J_1} \sin(x_4)$$

$$\dot{x}_4 = \left(\frac{M_2 g r}{J_2} - \frac{k_s r^2}{4J_2} \right) \sin(x_2) + \quad (25)$$

$$- \frac{k_s r}{2J_2} (l-b) + \frac{\tau_2}{J_2} + \frac{k_s r^2}{4J_2} \sin(x_3)$$

where, $g=9.81 \text{ m/s}^2$ is the gravitational acceleration constant. As given in Table 1, since $b < l$, the two pendulums repel each other in the upright position. The model introduced in this section has been studied by Spooner and Passino [13], who discuss the decentralized adaptive control using radial basis neural networks.

In the simulation studies presented, the plant introduced is controlled by the proposed control scheme. The aim is to produce some control signals such that the application of which results in the observation of a sliding motion in the phase plane. As the controller, the architecture described by (1) is utilized with \underline{u}_A being as described in (3). The structure of the control system is illustrated in Fig. 2, in which the plant is in an ordinary feedback loop. Based on the tracking error vector, first the value of s_p is evaluated and this quantity is passed through the Ψ function to get the value of s_c , which is used in the dynamic adjustment mechanism. In evaluating the value of the quantity s_p , the slope parameter of the switching line (λ) has been set to unity for both controllers.

In practical implementations of control structures for trajectory control of mechatronic devices, a number of difficulties are encountered, which make it difficult to achieve an accurate trajectory tracking. The simulation studies carried out address these difficulties. The first difficulty to be alleviated is the existence of the observation noise. To study the effects of this situation, which is very likely to be encountered in practice, the information used by the controller is corrupted by a Gaussian distributed random noise having zero mean and variance equal to $0.33e-6$. The peak magnitude of the noise signal is within $\pm 1e-3$ with probability very close to unity. The second difficulty is the nonzero positional initial conditions. In order to demonstrate the reaching mode performance of the algorithm, the initial positional errors have been set to $\pi/4$ radians and $-\pi/6$ radians for the first and the second pendulum. The reference trajectory used in the simulations is depicted in Fig. 3.

It should be pointed out that once the error or the rate of error comes very close to zero, the adjustment mechanism is driven solely by the noise signal corrupting the observed state variables. Since the bound of perturbing signal is known, the update law described in (17) can be modified such that the adverse effects of noise driven parameter tuning activity are reduced. This can be achieved by utilizing a sufficiently hard threshold function given by (26). The value of threshold is denoted by n_b and has been set to $2e-3$ in the simulations. The modified form of the update equation in (17) is given in (27).

$$T(s_p) = \left(1 + \exp\left(-10^5(|s_p| - n_b)\right)\right)^{-1} \quad (26)$$

$$\dot{\underline{\phi}} = -K \left(\mu I + \rho \frac{\partial^2 J}{\partial \underline{\phi} \partial \underline{\phi}^T} \right)^{-1} \text{sgn} \left(\frac{\partial J}{\partial \underline{\phi}} \right) T(s_p) \quad (27)$$

As the Ψ relation, the following selection is made parallel to the remarks presented in the fourth section.

$$\Psi(s_p) = s_p \quad (28)$$

Furthermore, in order to reduce the chattering effect in the sliding mode, the function in (29) has been used instead of the sgn function in the dynamic strategy described in (27), and initially, the adjustable parameters are all set to the values given in (30).

$$\text{sgn}(\Psi(s_p)) \approx \frac{\Psi(s_p)}{|\Psi(s_p)| + 0.05} \quad (29)$$

$$\begin{bmatrix} \phi_{11}(0) \\ \phi_{12}(0) \\ \phi_{13}(0) \end{bmatrix} = \begin{bmatrix} \phi_{21}(0) \\ \phi_{22}(0) \\ \phi_{23}(0) \end{bmatrix} = \begin{bmatrix} -20 \\ -10 \\ 0 \end{bmatrix} \quad (30)$$

Under these conditions, the state tracking error graph in Fig. 4 is obtained. The trend in position and velocity errors clearly stipulate that the algorithm is capable of achieving

precise tracking objective with a sufficiently fast response characterized by λ . The applied control signals are depicted in Fig. 5, in which the smoothness of the signals is another important property. The motion in the phase plane is illustrated in Fig. 6, in which after a fast reaching mode, a sliding mode is enforced and is maintained by producing a suitable control signal. Lastly, the behaviors of the parameters of the two controllers are illustrated in Fig. 7, from which the bounded evolution is clear.

During the simulations, the bounds for the uncertainties denoted by K for both pendulums have been set to 800. The weight parameters μ and ρ have been selected as unity for both controllers. These values of the design parameters have been chosen by trial-and-error approach, which is typically the case, as we do not have the values of the quantities on the right hand side of the inequality in (18). The simulation stepsize has been selected as 2.5 msec and the time required to perform the simulation has been measured as 36.562 seconds on a Pentium III-600 PC running Matlab 5.2 software. This indicates that the complexity of the algorithm in real time control applications is dependent on the speed of the chosen DSP interface, the widespread examples of which operates machine coded algorithms and performs thousands of floating point operations in a few milliseconds as they do not have to run an operating system.

V. CONCLUSIONS

In this paper, a novel method for establishing a sliding motion in the dynamics of a nonlinear plant is discussed. The method is based on the adoption of a nonlinear dynamic adjustment strategy in a controller structure, whose output is a linear in the adjustable parameters. The task is to drive the tracking error vector to the sliding manifold and keep it on the manifold forever. What makes the proposed algorithm so attractive in this sense is the fact that the sliding mode control of the plant is achieved while an equivalent regime is imposed on the controller parameters. Contrary to what is known in the field of variable structure controller design, the governing equations of the plant under control are assumed to be unknown and the lack of this knowledge is left as a difficulty to be alleviated by a learning controller.

As discussed throughout the paper, the problems that arise due to the uncertainties are alleviated by incorporating the robustness provided by the VSS technique into the proposed approach. A further attractiveness of the algorithm is the fact that the controller for each pendulum possesses only three adjustable parameters for the application example considered. The computational requirement is not therefore excessive. Fig. 8 depicts the required number of floating point operations (flops) for the controller performing one forward pass for control calculation and one backward pass for parameter tuning. Clearly the system studied in this work requires 2×246 flops which is affordable even for average speed embedded microprocessors.

Finally, the simulation results presented demonstrate that the algorithm discussed is able to compensate deficiencies caused by the imperfect observations of the state variables,

large initial errors and complex plant dynamics. From these points of view, the method proposed is highly promising in control engineering practice.

VI. REFERENCES

- [1] R. N. Sanner and J. J. E. Slotine, "Gaussian Networks for Direct Adaptive Control," *IEEE Transactions on Neural Networks*, Vol.3, No.6, pp. 837-863, 1992.
- [2] H. Sira-Ramirez and E. Colina-Morles, "A Sliding Mode Strategy for Adaptive Learning in Adalines", *IEEE Transactions on Circuits and Systems - I: Fundamental Theory and Applications*, Vol. 42, No.12, pp. 1001-1012, December 1995.
- [3] L. Hsu and J. A. Real, "Dual Mode Adaptive Control Using Gaussian Neural Networks," *Proc. of the 36th Conference on Decision and Control*, (CDC), New Orleans, LA, pp.4032-4037, 1997.
- [4] L. Hsu and J. A. Real, "Dual Mode Adaptive Control," *Proc. of the IFAC'99 World Congress*, Beijing, Vol. K, pp. 333-337, 1999.
- [5] X. Yu, M. Zhihong and S. M. M. Rahman, "Adaptive Sliding Mode Approach for Learning in a Feedforward Neural Network," *Neural Computing & Applications*, Vol. 7, pp. 289-294, 1998.
- [6] G. G. Parma, B. R. Menezes and A. P. Braga, "Sliding Mode Algorithm for Training Multilayer Artificial Neural Networks," *Electronics Letters*, Vol. 34, No. 1, pp. 97-98, January 1998.
- [7] H. Sira-Ramirez, E. Colina-Morles and F. Rivas-Echeverria, "Sliding Mode-Based Adaptive Learning in Dynamical-Filter-Weights Neurons," *International Journal of Control*, Vol.73, No.8, pp.678-685, 2000.
- [8] M. O. Efe, O. Kaynak and X. Yu, "Sliding Mode Control of a Three Degrees of Freedom Anthropoid Robot by Driving the Controller Parameters to an Equivalent Regime," *Transactions of the ASME: Journal of Dynamic Systems, Measurement and Control.*, Vol.122, No.4, pp.632-640, December 2000.
- [9] M. O. Efe and O. Kaynak, "On Stabilization of Gradient Based Training Strategies for Computationally Intelligent Systems," *IEEE Transactions on Fuzzy Systems*, Vol.8, No.5, pp.564-575, October 2000.
- [10] M. O. Efe, O. Kaynak and B. M. Wilamowski, "Stable Training of Computationally Intelligent Systems By Using Variable Structure Systems Technique," *IEEE Transactions on Industrial Electronics*, Vol.47, No.2, pp.487-496, April 2000.
- [11] O. Kaynak, K. Erbatur and M. Ertugrul, "The Fusion of Computationally Intelligent Methodologies and Sliding-Mode Control – A Survey," *IEEE Transactions on Industrial Electronics*, Vol. 48, No.1, pp.4-17, February 2001.
- [12] M. O. Efe, Variable Structure Systems Theory Based Training Strategies for Computationally Intelligent Systems, Ph.D. Thesis, Bogazici University, 2000.
- [13] J. T. Spooner and K. M. Passino, "Decentralized Adaptive Control of Nonlinear Systems Using Radial Basis Neural Networks," *IEEE Trans. on Automatic Control*, v.44, no.11, pp. 2050-2057, 1999.

Table 1. Plant Parameters

Mass of pend. 1	M_1	2 kg
Mass of pend. 2	M_2	2.5 kg
Moment of inertia for pend. 1	J_1	0.5 kg
Moment of inertia for pend. 2	J_2	0.625 kg
Spring constant	k_s	100 N/m
Natural length of the spring	l	0.5 m
Distance between pend. hinges	b	0.4 m
Pendulum height	r	0.5 m

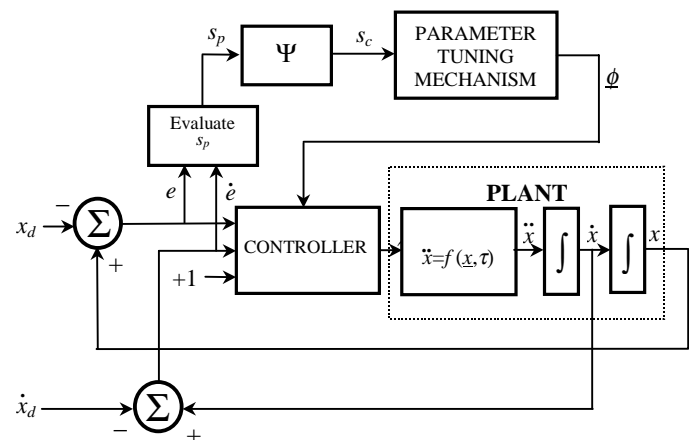


Fig. 1. Structure of the control system

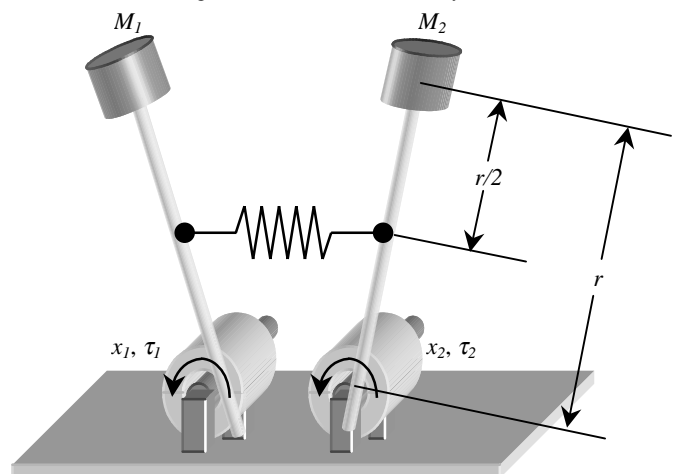


Fig. 2. Physical structure of the double pendulum system

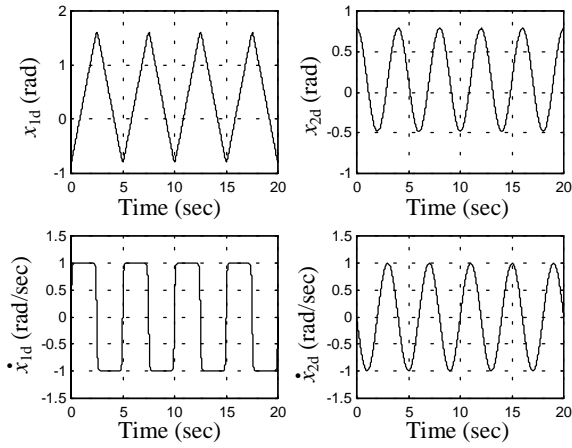


Fig. 3. Reference state trajectories

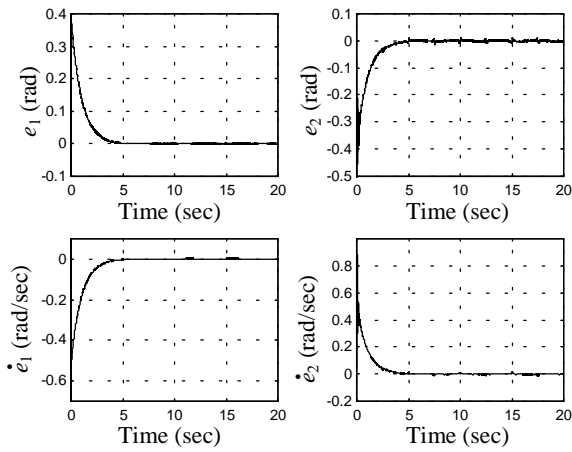


Fig. 4. State tracking errors

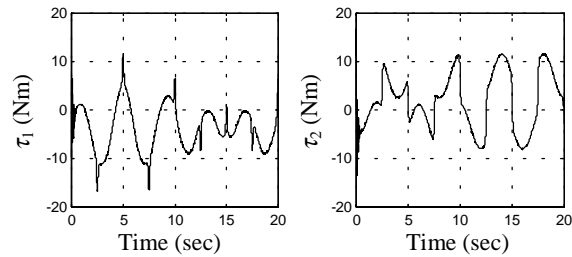


Fig. 5. Applied control signals

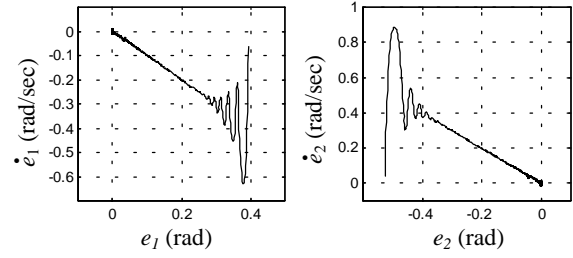


Fig. 6. Trajectories in the phase plane

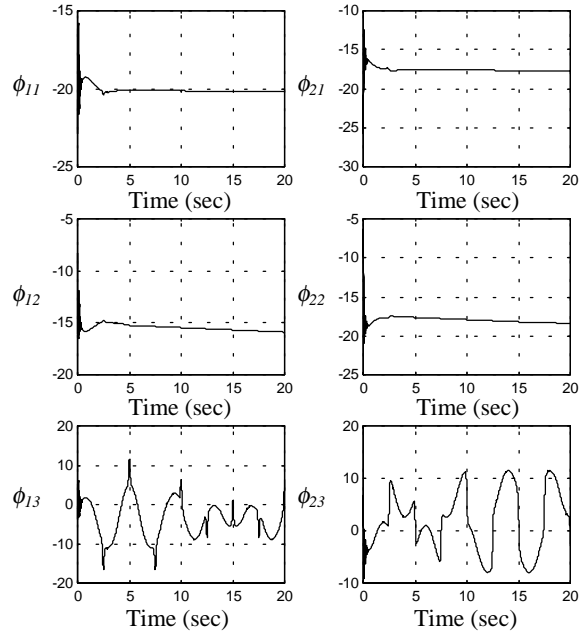


Fig. 7. Evolution of the parameters of the controllers

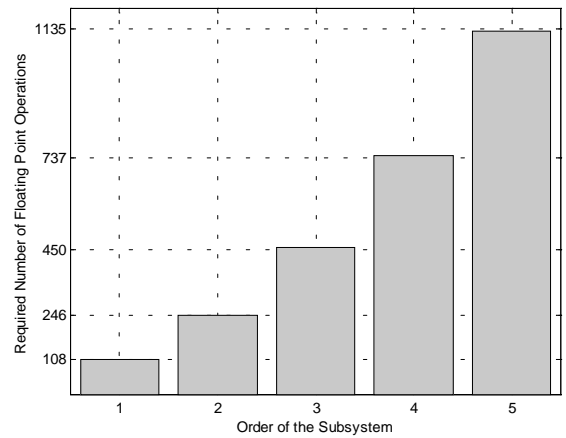


Fig. 8. Computational burden of the approach